Biomechanical properties of human T cells in the process of activation based on diametric compression by micromanipulation

Du, Mingming; Kalia, Neena; Frumento, Guido; Chen, Frederick; Zhang, Zhibing

DOI:
10.1016/j.medengphy.2016.11.011

Biomechanical properties of human T cells in the process of activation based on diametric compression by micromanipulation

Mingming Du[1], Neena Kalia[2], Guido Frumento[3,4], Frederick Chen[3,4*], Zhibing Zhang [1,*]

[1] *School of Chemical Engineering, University of Birmingham, Birmingham B15 2TT, UK*

[2] *Institute of Cardiovascular Sciences, University of Birmingham, Birmingham B15 2TT, UK*

[3] *Institute of Immunogy and Immunotherapy, University of Birmingham, Birmingham B15 2TT, UK*

[4] *NHS Blood and Transplant, Vincent Drive, Birmingham B15 2SG*

***Authors for correspondence: Email: z.zhang@bham.ac.uk and frederick.chen@nhsbt.nhs.uk**

Abstract

A crucial step in enabling adoptive T cell therapy is the isolation of antigen (Ag)-specific $CD8^+$ T lymphocytes. Mechanical changes that accompany $CD8^+$ T lymphocyte activation and migration from circulating blood across endothelial cells into target tissue, may be used as parameters for microfluidic sorting of activated $CD8^+$ T cells. $CD8^+$ T cells were activated in vitro using anti-CD3 for a total of 4 days, and samples of cells were mechanically tested on day 0 prior to activation and on day 2 and 4 post-activation using a micromanipulation technique. The diameter of activated $CD8^+$ T cells was significantly larger than resting cells suggesting that activation was accompanied by an increase in cell volume. While the Young's modulus value as determined by the force versus displacement data up to a nominal deformation of 10% decreased after activation, this may be due to the activation causing a weakening of the cell membrane and cytoskeleton. However, nominal rupture tension determined by compressing single cells to large deformations until rupture, decreased from day 0 to day 2, and then recovered on day 4 post-activation. This may be related to the mechanical properties of the cell nucleus. These novel data show unique biomechanical changes of activated $CD8^+$ T cells which may be further exploited for the development of new microfluidic cell separation systems.

Key words T lymphocytes; Activation; Cell Separation; Mechanics; Micromanipulation

Introduction

Cell-based therapies have witnessed tremendous expansion in the past two decades, from curative haematopoietic stem cell transplantation for leukemias to adoptive antigen (Ag)-specific $CD8^+$ T cell immunotherapies of viral infections and cancers. $CD8^+$ T cells for adoptive immunotherapies can be generated through *in vitro* expansion or immunomagnetic isolation of pre-existing Ag-specific lymphocytes from blood or tumor-infiltrating lymphocytes. The former method has the drawback of driving T cells to exhaustion through repeated cycles of *in vitro* antigen stimulation and expansion, which ultimately impacts on their efficacy to eliminate tumour or infected cells [1]. This is in contrast to direct *ex vivo* selection which requires minimal manipulation and thus retains the proliferative capacity and therapeutic functionality of the lymphocytes.

For this reason, immunomagnetic selection of fresh *ex vivo* cells has been adopted in recent clinical trials where a small number of pre-existing circulating virus-specific $CD8^+$ T cells can be directly selected from donor blood to target viral infections and tumours in stem cell transplant patients [2-4]. This method has been used to treat cytomegalovirus, Epstein–Barr virus and adenovirus infections, and also lymphomas such as post-transplant lymphoproliferative disorder. Immunomagnetic selection systems utilize antibody or ligand-recognition of unique phenotypic markers on the cell surface to separate cells. With the recent breakthrough in utilising T cells expressing the CD19-specific chimeric antigen receptor (CAR) for the treatment of B cell acute lymphoblastic leukaemia [5], selection of Ag-specific cells could also become a key purification step in the *in vitro* expansion of immunoreceptor engineered cells.

However, there are limitations to immunomagnetic methods with regards to the loss of low frequency cells through multiple processing steps such as washes and sub-optimal purity and recovery from the selection itself, and not least, the costs of the specialized GMP reagents. An alternate approach to immunomagnetic isolation, is to select cells using clinical grade fluorescence-activated cell sorting (FACS) [6-8]. Though highly sensitive and specific, FACS sorting of rare cells (<1%) to therapeutic quantities, is time consuming and associated with the risk of reduced cell viability [9].

The biophysical properties of cells also allow different cell types to be discriminated. For example, in flow cytometry the cell size determines light scattering properties, and in apheresis, centrifugal forces separate blood into its constituent cellular components based on physical properties. An emerging technique based on microfluidic separation utilizes the biophysical properties of live cells by applying different hydrodynamic forces on the target particles or by utilizing the natural biomechanical variation of the cells to guide them into different flow paths [10]. Studies reporting cell sorting based on size or stiffness demonstrate the potential applications of the microfluidic cell sorting technique for separating tumor cells, erythrocytes as well as activated Ag-specific T cells [11-14]. It should therefore be possible to use natural or induced variations in biomechanical properties to separate activated lymphocytes from non-activated lymphocytes and other cell types.

However, before we can utilize microfluidic assays to separate lymphocytes for clinical therapeutic purposes, a more precise study of their biomechanical properties is needed.

Parameters such as cell rigidity and deformability can be measured using several techniques including atomic force microscopy (AFM), micromanipulation, magnetic tweezers, micropipette aspiration, optical tweezers, shear flow, cell stretching and microelectromechanical systems [15]. Powerful techniques such as AFM have previously been used to measure the elastic properties of lymphocytes, but only deform a portion of the cell surface (nano-indentation) and so do not measure the mechanical properties of the whole cell [16]. However, circulating lymphocytes experience significant repeated hydrodynamic and mechanical stresses in blood vessels, which are applied along their entirety leading to large deformations in the microcirculation. These are particularly seen following lymphocyte activation when they transmigrate out of blood vessels into the surrounding interstitial tissue. Therefore, it is important to understand the mechanical properties of lymphocytes under large, as well as small, deformations. Of the techniques mentioned, micromanipulation, based on the compression of single cells between two parallel surfaces, can be used to generate small to large deformations of cells, including deformations where they rupture, which is appropriate for the purpose [17].

We report the first study that uses the micromanipulation technique to measure the temporal biomechanical changes of $CD8^+$ T cells following Ag-induced stimulation. Moreover, the studies were conducted on live cells rather than fixed cells. We have determined mechanical strength parameters such as rupture force, rupture deformation and nominal rupture stress/tension for resting (unactivated) and activated T cells compressed to rupture. We have also modeled the compression data of T cells

corresponding to smaller deformations to obtain a measure of the elasticity, defined as the Young's modulus. This work provides important new data on the biomechanics of activated $CD8^+$ T cells which can be used for future development of microfluidic separation of cells that have selectively responded to specific antigen stimulation.

Materials and Methods

Isolation, culture and *in vitro* activation of T lymphocytes

Peripheral blood was collected from three healthy drug-free adult donors after informed consent. Peripheral blood mononuclear cells (PBMC) were isolated by Ficoll separation. The contaminating erythrocytes were removed by osmotic lysis. Briefly, 1 ml of distilled water was added to the cell pellet. After 30s, 14 ml of RPMI 1640 (Sigma-Aldrich, St. Louis, MO, USA) was added, and the cells were washed once. Untouched $CD8^+$ T lymphocytes were isolated by negative immunomagnetic selection, using CD8+ T Cell Isolation Kit and LS columns (Miltenyi Biotec, Bergisch Gladbach, Germany), following the manufacturer's instructions. Cell purity was checked using a FacsCanto II flow cytometer (BD, San Jose, CA, USA) and in all the cases the $CD8^+$ T lymphocyte purity was above 90%. Enriched $CD8^+$ T lymphocytes were resuspended in RPMI 1640 plus 10% foetal calf serum (Sigma-Aldrich, UK). Some cells were activated by culturing in the presence of 30 ng/mL anti-CD3 antibody OKT3 (BioLegend, San Diego, CA, USA) plus 600 U/mL IL-2 (Chiron, Emeryville, USA). For control samples, the non-activated

139 $CD8^+$ T cells were cultured in the medium for up to 4 days, and they were mechanically
140 tested on Day 0, Day 2 and Day 4.
141
142 **Micromanipulation technique**
143
144 The mechanical properties of resting and activated $CD8^+$ T lymphocytes were measured
145 either immediately after harvesting (day 0) or tested 2 days or 4 days post-activation.
146 Cells were diluted with phosphate buffered saline to reduce cell density in suspension
147 and mechanical testing was completed within 3 hours using a well established
148 micromanipulation technique, the principle and details of which have been previously
149 described [17, 18]. Briefly, the technique involves compression of a single cell between
150 the flat end of a probe and the bottom of a glass chamber containing the culture
151 medium (**Figure 1**). A microscopic image of a single mammalian cell under
152 compression is presented in [18]. Suspended single cells were allowed to settle to the
153 bottom of the chamber, and images were captured with a side-view high-speed digital
154 camera. A probe with a 25 μm diameter was driven down by a stepping motor towards
155 the single cells. The probe was connected to a force transducer (406A-ER, Aurora
156 Scientific Inc. Canada) in order to collect the data of instantaneous force imposed on
157 single cells at a frequency of 50 Hz.
158
159 **Determination of activation-related changes in cell size**
160

The diameter of $CD8^+$ T cells was directly measured from their images on a TV monitor which was connected with the side view camera on the micromanipulation rig. The magnification of the camera had been pre-calibrated, and the measurement of cell diameter was accurate to ± 0.1μm. The cell size was also evaluated by flow cytometry. The enriched $CD8^+$ T lymphocytes were stained with anti CD3/PE and 7AAD (BD). The forward scatter (FSC-A) value of the 7AAD-/CD3+ cells was recorded using the FacsCanto II flow cytometer (BD, San Jose, CA, USA).

Determination of rupture force, rupture deformation, nominal rupture stress and nominal rupture tension

Single cells from each of the 3 donor samples were selected randomly and compressed to large deformations until they ruptured using a probe at the speed of 2μm/s. The numer of cells taken from each sample was 20 in order to give statistically representative results. The force (μN) imposed on the cell was plotted against the distance (μm) the probe moved towards the glass chamber (force vs displacement). These graphs were then used to determine the mean rupture force and the percentage (%) deformation at rupture for resting and activated cells. The % rupture deformation was calculated as the ratio of the displacement value at rupture to the initial diameter of the cell.

Nominal rupture stress (σ_R) was calculated as the ratio of the rupture force to the initial cross-sectional area of the cell. Nominal rupture tension (T_R) was calculated as the

ratio of the rupture force to the initial diameter of the cell. These values provide a comparable indication of the mechanical strength of cells and were calculated using Equations (1) and (2) respectively, where F_R is the rupture force and *d* is the original diameter of the single cell before compression.

$$\sigma_R = \frac{4F_R}{\pi d^2} \quad (1)$$

$$T_R = \frac{F_R}{d} \quad (2)$$

Determination of the Young's Modulus

Theoretically, the Hertz model is valid and commonly used to describe the relationship between the imposed force and displacement for small deformations of an elastic object, which has been successfully applied to determination of the Young's Modulus of different particles including cells when compressed to a small deformation [19-21]. The experimental force versus displacement data up to a nominal deformation of 10% were fitted to Equation (3), similar to the approach described in [20] to determine the Young's modulus of T cells, having presumed that the individual cells were homogeneous, incompressible, elastic spheres and that there was no friction at the cell-substrate interfaces.

$$F = \frac{E^* \sqrt{2R}}{3(1-\upsilon^2)} \delta^{3/2} \quad (3)$$

where F is the applied force, E is the Young's modulus of the cell, R is the original cell radius, ν is the Poisson's ratio of the cell and δ is the diametric compressive displacement. From the model, there should be a linear relationship between F and $\delta^{3/2}$. From the slope of the linear fitting, cell radius and Poisson ratio (assumed to be 0.5 since the cells are assumed to be incompressible), the value of Young's modulus was determined - higher values indicate cells that are less deformable for a given applied force and vice versa.

Statistical analysis

Values for the mechanical property parameters of the lymphocytes are presented as mean ± standard error. Paired Student t-tests were performed to determine significant differences among the mechanical properties of different samples, with statistical significance reported at the 95% confidence level ($p<0.05$).

Results

Activation of $CD8^+$ T lymphocytes increases their cell size

The diameter of the single cells was measured from their images using the side-view camera on the micromanipulator. The diameter of resting CD8+ T cells (day 0) was 6.1 ± 0.6 µm. This increased significantly ($p<0.05$) upon activation to 9.7 ± 1.1 µm on day 2 post-activation and remained significantly ($p<0.05$) greater on day 4 post-activation when compared to resting cell values (**Figure 2a)**. There was no significant difference between the activated samples at day 2 and day 4 post-activation. Changes in cell diameter are also shown by the data generated using flow cytometry (**Figure 2b**). The FSC-A value of resting T cells are again significantly greater on day 2 ($p<0.05$) and day 4 post-activation ($p<0.05$) when compared to resting cell values. Interestingly, it was noted that CD8+ T cells that had been activated and tested on day 2 post-activation tended to 'stick' to the force transducer probe (image not shown), possibly indicating some change in their adhesive nature in the early stages of activation.

Compression curves of T cells to rupture

Micromanipulation studies demonstrated that the individual CD8+ T cells tested in the same sample were heterogeneous in their diameter and their force versus displacement curves even for single cells of same diameter, however, all tested single cells showed common characteristics in their compression curves. Typical curves showing the relationship between the force and displacement during continuous diametrical compression of a single lymphocyte to rupture at day 0, 2 and 4 days post-activation are shown in **Figures 3a-c**. At point A, the probe started to touch the cell, and the resistant force increased until point B where the cell ruptured. As a result of rupture, the force

241 decreased rapidly to point C, followed by curve CD where the force increased
242 continuously which represents the compression of cell debris until the probe touched
243 bottom of the glass chamber.

244

245 **Rupture force increases at 4 days post-activation**

246 The mean cell rupture force (μN) was determined from the force vs displacement curves
247 (*y*-axis value at point B). The rupture force was similar between the resting (day 0) and
248 activated cells at 2 days post-activation with mean values of 2.3 ± 0.8 μN and 2.6 ± 0.9
249 μN respectively. However, when activated cells were analyzed at 4 days, the rupture
250 force significantly ($p<0.05$) increased to 4.6 ± 1.6 μN ($p<0.05$) when compared to resting
251 cells (**Figure 4a**). The % rupture deformations of resting T lymphocytes and activated
252 lymphocytes at 2 and 4 days post-activation was not significantly different with mean
253 values of 78.3 ± 1.3%, 79.7 ± 1.6% and 77.5 ± 1.5% obtained respectively (**Figure 4b**).

254

255 **Nominal rupture stress / tension decreases at 2 days post-activation**

256 The nominal rupture tension significantly ($p<0.05$) decreased from 0.58 ± 0.07 N/m for
257 resting cells to 0.45 ± 0.07 N/m for cells at 2 days post-activation. This increased to
258 0.62 ± 0.10 N/m on day 4 post-activation, a value not significantly different to resting
259 cells (**Figure 5**). A similar pattern was observed for nominal rupture stress (**Figure 5**).

260

261 **Young's modulus decreases in activated $CD8^+$ T cells**

The Young's modulus was calculated from data obtained corresponding to small deformations of T cells. Typical force versus displacement data with a linear fit based on the Hertz model for cells at day 0, 2 and 4 days post-activation are shown in **Figures 6a-c**. Mean correlation coefficient values of 0.84±0.05, 0.85±0.04 and 0.85±0.06 were obtained for resting cells and cells at 2 days post-activation and 4 days post-activation respectively. The values of Young's modulus decreased significantly at both 2 days post-activation ($p<0.05$) and 4 days post-activation ($p<0.05$) when compared to resting cells at day 0 (**Figure 6d**). Actual calculated mean values for the Young's Modulus were 58.0 ± 6.3 kPa, 43.7± 5.0 kPa, and 43.0± 6.3 kPa for T lymphocytes at day 0, day 2 post-activation and day 4 post-activation respectively. There was no significant difference in the mean Young's modulus between T cells activated for 2 days and 4 days ($p>0.05$).

No change in the mechanical properties of non-activated CD8+ T cells for up to 4 days

The diameter of non-activated T cells did not change significantly upon incubation on day 2 and day 4 when cultured in the medium (Figure 7a). There was also no significant difference in the nominal rupture tension/stress between the resting samples, as shown in Figure 7b.

Discussion

This novel study analysed the biomechanical properties of live lymphocytes undergoing activation using a micromanipulation technique, without the need for fixing the cells.

Mammalian cells can show heterogeneity in their biomechanical property parameters, which is reflected in the standard error of the mean, and 3 donors should give reasonably representative results [22]. An increase in cell volume was observed as a result of activation at both 2 and 4 days post-activation. An initial fall in whole cell mechanical strength was observed at 2 days post-activation as indicated by the decreased rupture stress/tension values. Thereafter, although lymphocytes remained bigger, they regained their mechanical strength at day 4 post-activation, possibly reflecting the tailing off of activation and cellular recovery. However, the Young's modulus at small deformations (up to 10%), decreased at both 2 and 4 days post-activation suggesting the outer membrane became and remained flexible. This is the first time, as far as we are aware, that a micromanipulation technique has been used to directly analyze the biomechanical properties including rupture strength of human T cells at various time points post-activation. A summary of the data obtained are provided in Table 1 below.

Table 1: Change in the mechanical properties of human T cells at 2 days and 4 days post-activation

All values compared to resting cells	*Cell size*	*Rupture force*	*% rupture deformation*	*Rupture stress and tension*	*Young's modulus*
2 days post-activation	↑	–	–	↓	↓
4 days post-activation	↑	↑	–	–	↓

The rupture force for activated cells at 4 days post-activation was significantly greater than resting and activated cells at 2 days post-activation. At first glance, this suggested these cells were “stronger”, thus requiring the greater force to rupture. However, this data did not take into account that the size of the cells was different for the three groups which could explain their differing rupture force. Increases in CD8+ T cell size at similar time points have previously been described microscopically post-OKT3 activation [23, 24] and occurs so that activated lymphocytes can duplicate their contents and divide. To make comparisons between the mechanical properties of resting and activated cells, nominal rupture stress and tension was calculated, which took into account the initial cross-sectional area and diameter of the cells. It should be pointed out that the initial cross-sectional area may be different from the real contact area between the force probe or bottom substrate and cell at rupture, and the latter depends on the deformation at rupture. As Figure 3b shows, the deformation at rupture did not change significantly up to 4 days, the choice of using nominal rupture stress for comparison is still valid. Once corrected for size, it became apparent that resting cells and cells at 4 days post-activation were equally strong but more than cells at 2 days post-activation. Hence the nominal stress/tension data indicated that $CD8^+$ T lymphocytes became weaker early during activation, while their mechanical strength was regained 4 days later. The higher mechanical strength of the resting lymphocytes is essential functionally to maintain sufficient integrity and thus protect them from damage by the significant hydrodynamic and mechanical stresses exerted on them in the circulation [25]. Following stimulation by Ag-presenting cells *in vivo*, CD8+ T cells move out of the circulation to the site of

infection where they acquire cytolytic effector activity against the pathogen. Therefore, the initial weakened cellular strength observed in this study may functionally correlate with, and enable, the transmigration of circulating lymphocytes between endothelial cells into tissue. After this event, lymphocytes regain their original form and strength for mediating effector activity and this functionally correlates with the higher nominal rupture stress/tension observed at 4 day post-activation than day 2.

Previous studies have shown that the nucleus of T lymphocytes is approximately 5 times stiffer than the cytoplasm and occupies about 80% of the cell [26]. This characteristic makes T lymphocytes different from other eukaryocyte cells (mesenchymal cells, endothelial cells, etc.) in which the cell nucleus only occupies ~10% of the cell volume [27]. When faced with higher compressive forces, the lymphocyte cell nucleus therefore plays an increasingly significant role in resisting the applied force for the whole cell. The reduced nominal rupture stress / tension at 2 days post-activation indicates the cell nucleus, as well as the cell membrane and cytoskeleton of these larger cells, may have become less strong. However, at the later stage of activation (from day 2 to day 4), these structures regained their mechanical strength while cell volume remained unchanged during this time.

At lower applied force, which compresses the cell to a smaller deformation, the mechanical stiffness of T cells is governed primarily by the membrane which is considered to be largely elastic. The Young's modulus is a measure of the intrinsic stiffness of an elastic material undergoing recoverable compression. The Hertz model

was able to determine the Young's modulus of T lymphocytes at small deformations (up to 10%), hence providing an indication of the elasticity of the outer region (cell membrane and cytoskeleton) of the cell. Although the noise to signal ratio is relatively big corresponding to small deformations, significant differences between samples were still demonstrated from the values of Young's Modulus. The results indicate that depolymerization or reorganization of cytoskeleton polymers probably happened when the cells were activated, resulting in softness of the outer cortex during the 4 days. From the rupture parameters at large deformation and the Young's Modulus calculated at small deformation, we hypothesized that the cytoskeleton remained less stiff post-activation, while the nucleus regained rigidity during the 4 days activation, which remains to be validated in future. In the calculation of Young's modulus, for living cells, the Poisson ratio is typically between 0.4 and 0.5, which means they are mostly or fully incompressible [28]. A value of 0.5 is chosen here since the Poisson ratio of $CD8^+$ T lymphocytes has not been studied. Moreover, from the Hertz model (Eq. 3), it can be seen that Poisson ratio (ν) has little effect on Young's modulus that increases by only 12% when ν varies from 0.4 to 0.5. For measuring the local Young's modulus of the cell membrane with greater sensitivity, and its spatial distribution, AFM may be used which can measure the forces in the order of pico-Newton to nano-Newton.

Conclusions

Using biomechanical properties in microfluidic cell sorting is increasingly recognized as a marker-free way to separate biological cells. With the increasing interest in using CD8+ T cells for therapeutic purposes, a separation method in which cells remain unperturbed is important if they are to be transplanted after mechanical characterization and sorting. This study utilizes the micromanipulation technique, a relatively straightforward method to evaluate the mechanical property changes of activated CD8+ T lymphocytes. It has been found that there was no significant change in the mechanical property parameters including cell size, nominal rupture stress and rupture tension of non-activated CD8+ T cells in the culture medium for up to 4 days, which is in clear contrast to those activated in vitro using anti-CD3. The activated cells showed a significant increase in size and decrease in rupture stress/tension at day 2 but the mechanical strength recovered at day 4.The data obtained on size and mechanical properties post-activation may be utilized for developing microfluidic devices for their separation. Furthermore, this work obtains complementary data for CD8+ T cells circulating *in vivo* with respect to adapting to the mechanical barriers. The ability to directly measure the biomechanical properties of live lymphocyte subsets not only facilitates the development of a cell separation system based on defined physical properties of cells but also provides a 'biomarker' for assessing the physical state of lymphocytes, that could be used for assessing quality after bioprocessing of cells eg. cryopreservation.

.

Acknowledgments

This study is sponsored by a joint Li Siguang Scholarship from the University of Birmingham, UK and the China Scholarship Council.

References

[1] Klebanoff CA, Gattinoni L, Restifo NP. Sorting through subsets: Which T cell populations mediate highly effective adoptive immunotherapy? J Immunol 2012;35:651.

[2] Peggs KS, Verfuerth S, Pizzey A, Khan N, Guiver M, Moss PA, et al. Adoptive cellular therapy for early cytomegalovirus infection after allogeneic stem-cell transplantation with virus-specific T-cell lines. The Lancet. 2003;362:1375-7.

[3] Feuchtinger T, Matthes-Martin S, Richard C, Lion T, Fuhrer M, Hamprecht K, et al. Safe adoptive transfer of virus-specific T-cell immunity for the treatment of systemic adenovirus infection after allogeneic stem cell transplantation. Br J Haematol 2006;134:64-76.

[4] Moosmann A, Bigalke I, Tischer J, Schirrmann L, Kasten J, Tippmer S, et al. Effective and long-term control of EBV PTLD after transfer of peptide-selected T cells. Blood. 2010;115:2960-70.

[5] Davila ML, Riviere I, Wang X, Bartido S, Park J, Curran K, et al. Efficacy and toxicity management of 19-28z CAR T cell therapy in B cell acute lymphoblastic leukemia. Sci Transl Med 2014;6:224ra25-ra25.

[6] Cepok S, Zhou D, Srivastava R, Nessler S, Stei S, Büssow K, et al. Identification of Epstein-Barr virus proteins as putative targets of the immune response in multiple sclerosis. J Clin Invest 2005;115:1352-1360.

[7] Kodituwakku AP, Jessup C, Zola H, Roberton DM. Isolation of antigen-specific B cells. Immunol Cell Biol 2003;81:163-70.

[8] Sung J, Yang H-M, Park J, Choi G-S, Joh J-W, Kwon C, et al. Isolation and characterization of mouse mesenchymal stem cells. Transplant Proc 2008; 40:2649-54.

[9] Wulff S, Martin K, Vandergaw A, Boenisch T, Brotherick I, Hoy T, et al. DakoCytomation - Guide to Flow Cytometry. 2006.

[10] Tsutsui H, Ho C-M. Cell separation by non-inertial force fields in microfluidic systems. Mech Res Commun 2009;36:92-103.

[11] Lim CT, Hoon DSBH. Circulating tumor cells: Cancer's deadly couriers. Physics Today 2014; 67: 26-30..

[12] Hou HW, Bhagat AAS, Chong AGL, Mao P, Tan KSW, Han J, et al. Deformability based cell margination—a simple microfluidic design for malaria-infected erythrocyte separation. Lab Chip 2010;10:2605-13.

[13] Hur SC, Henderson-MacLennan NK, McCabe ER, Di Carlo D. Deformability-based cell classification and enrichment using inertial microfluidics. Lab Chip 2011;11:912-20.

[14] Preira P, Grandne V, Forel J-M, Gabriele S, Camara M, Theodoly O. Passive circulating cell sorting by deformability using a microfluidic gradual filter. Lab Chip 2013;13:161-70.

[15] Neubauer MP, Poehlmann M, Fery A. Microcapsule mechanics: From stability to function. Adv Colloid Interface Sci 2014;207:65-80.

[16] Cai X, Xing X, Cai J, Chen Q, Wu S, Huang F. Connection between biomechanics and cytoskeleton structure of lymphocyte and Jurkat cells: An AFM study. Micron. 2010;41:257-62.

[17] Nguyen BV, Wang QG, Kuiper NJ, El Haj AJ, Thomas CR, Zhang Z. Biomechanical properties of single chondrocytes and chondrons determined by micromanipulation and finite-element modelling. J R Soc Interface 2010;7:1723-33.

[18] Nguyen BV, Wang Q, Kuiper NJ, El Haj AJ, Thomas CR, Zhang Z. Strain-dependent viscoelastic behaviour and rupture force of single chondrocytes and chondrons under compression. Biotechnol Lett 2009;31:803-9.
[19] Kuznetsova TG, Starodubtseva MN, Yegorenkov NI, Chizhik SA, Zhdanov RI. Atomic force microscopy probing of cell elasticity. Micron 2007;38:824-33.
[20] Yan Y, Zhang Z, Stokes JR, Zhou Q-Z, Ma G-H, Adams MJ. Mechanical characterization of agarose micro-particles with a narrow size distribution. Powder Technol 2009;192:122-30.
[21] Martens JC, Radmacher M. Softening of the actin cytoskeleton by inhibition of myosin II. Pflugers Arch, EJP 2008;456:95-100.
[22] Pleumeekers MM, Nimeskern L, Koevoet WLM, Kops N, Poublon RML, Stok KS, van Osch GJVM. The in vitro and in vivo capacity of culture-expanded human cells from several sources encapsulated in alginate to form cartilage. Eur Cell Mater 2014; 27: 264-280.
[23] Wu Y, Lu H, Cai J, He X, Hu Y, Zhao H, et al. Membrane surface nanostructures and adhesion property of T lymphocytes exploited by AFM. Nanoscale Res Lett 2009;4:942-7.
[24] Teague TK, Munn L, Zygourakis K, McIntyre BW. Analysis of lymphocyte activation and proliferation by video microscopy and digital imaging. Cytometry 1993;14:772-82.
[25] Brown MJ, Hallam JA, Colucci-Guyon E, Shaw S. Rigidity of circulating lymphocytes is primarily conferred by vimentin intermediate filaments. J Immunol 2001;166:6640-6.
[26] Friedl P, Wolf K, Lammerding J. Nuclear mechanics during cell migration. Curr Opin Cell Biol 2011;23:55-64.
[27] Tsien R, Pozzan T, Rink T. Calcium homeostasis in intact lymphocytes: cytoplasmic free calcium monitored with a new, intracellularly trapped fluorescent indicator. J Cell Biol 1982;94:325-34.
[28] Trickeya WR, Baaijensb FPT, Laursenc TA, Alexopoulosa LG, Farshid Guilaka F. Determination of the Poisson's ratio of the cell: recovery properties of chondrocytes after release from complete micropipette aspiration. J Biomech 2006; 39:78–87.

Figure Legends

Figure. 1. Schematic diagram of the micromanipulation rig: (1) Force transducer; (2) probe; (3) stepping motor; (4) computer with motor control and data acquisition system; (5) Bottom-view microscope; (6) side-view microscope; (7) high-speed camera; (8) single cells in phosphate buffered saline; (9) glass chamber.

Figure 2. Changes in the diameter of T lymphocytes was quantitated using (a) direct measurement of a microscopy image generated using the side-view camera on the micromanipulator and (b) flow cytometry. Both methods showed a similar significant increase in cell diameter as a result of T cell activation. N=3 donor samples for each group with 20 single cells, selected randomly from each sample. *$p<0.05$ as determined using a paired Student t-test.

Figure 3. Typical force-displacement curves obtained at a compression speed of 2μm/s for T cells to rupture on (a) day 0 prior to activation (resting cells) (b) day 2 post-activation and (c) day 4 post-activation. At point A, the probe touched the cell and the resistant force increased until point B where the cell ruptured. Rupture resulted in the force decreasing rapidly to point C, followed by curve CD where force increased until the probe touched bottom of the glass chamber. N=3 donor samples for each group with 20 single cells, selected randomly from each sample. *$p<0.05$ as determined using a paired Student t-test.

Figure 4. The (a) mean rupture force and (b) mean rupture deformation of T cells on (a) day 0 prior to activation (resting cells) (b) day 2 post-activation and (c) day 4 post-activation. The force required to rupture cells was larger for activated cells at 4 days post-activation. All cells were ruptured when they reached a % deformation close to 80%. N=3 donor samples for each group with 20 single cells, selected randomly from each sample. *p<0.05 as determined using a paired Student t-test.

Figure 5. The nominal rupture tension and nominal rupture stress of T cells on (a) day 0 prior to activation (resting cells) (b) day 2 post-activation and (c) day 4 post-activation. Both values significantly decreased for cells at 2 days post-activation. N=3 donor samples for each group with 20 single cells, selected randomly from each sample. *p<0.05 as determined using a paired Student t-test.

Figure 6. The typical linear fit (line) of the Hertz model to the obtained force-displacement data (o) for T cells compressed to small deformations on (a) day 0 prior to activation (resting cells) (b) day 2 post-activation and (c) day 4 post-activation. The mean values of the correlation coefficient are 0.84±0.05, 0.85±0.04 and 0.85±0.06 respectively with an overall range of 0.7 to 0.9. (d) The Young's modulus was calculated from these data, which decreased significantly as a results of activation. N=3 donor samples for each group with 20 single cells, selected randomly from each sample. *p<0.05 as determined using a paired Student t-test.

FIGURE 1

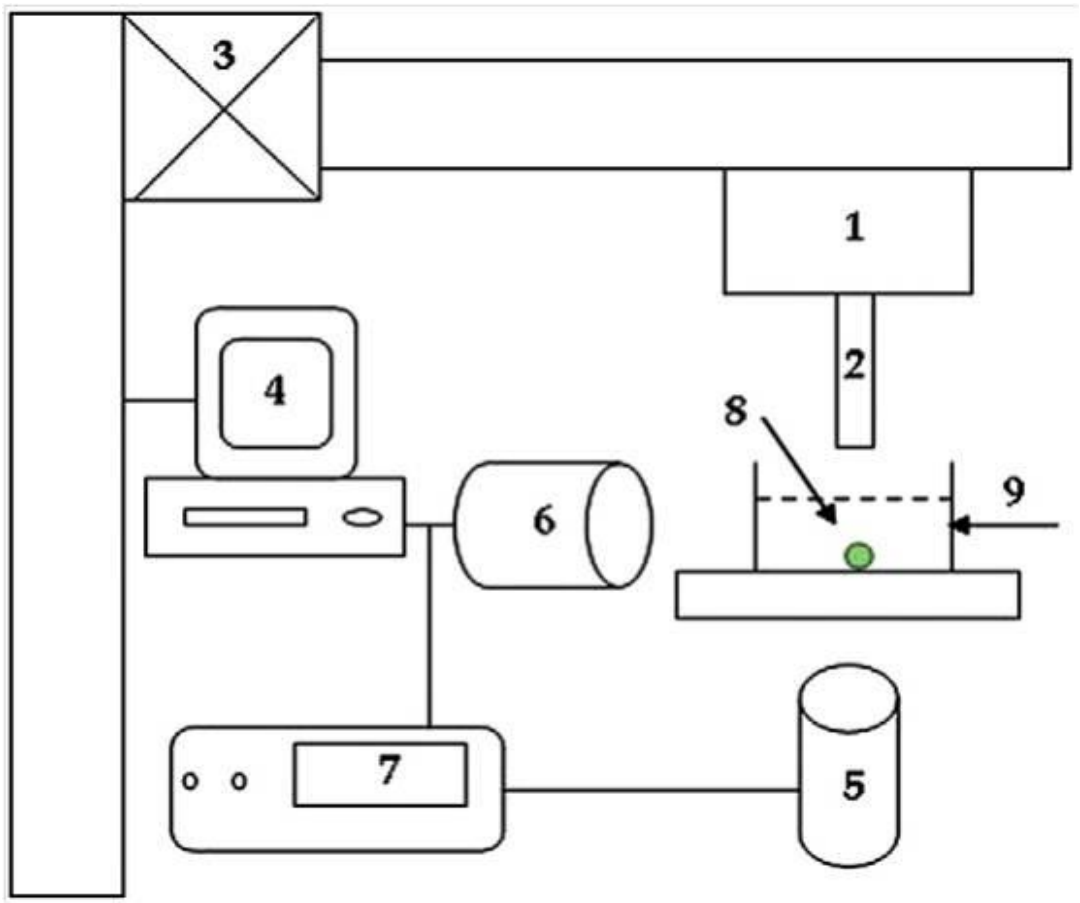

FIGURE 2

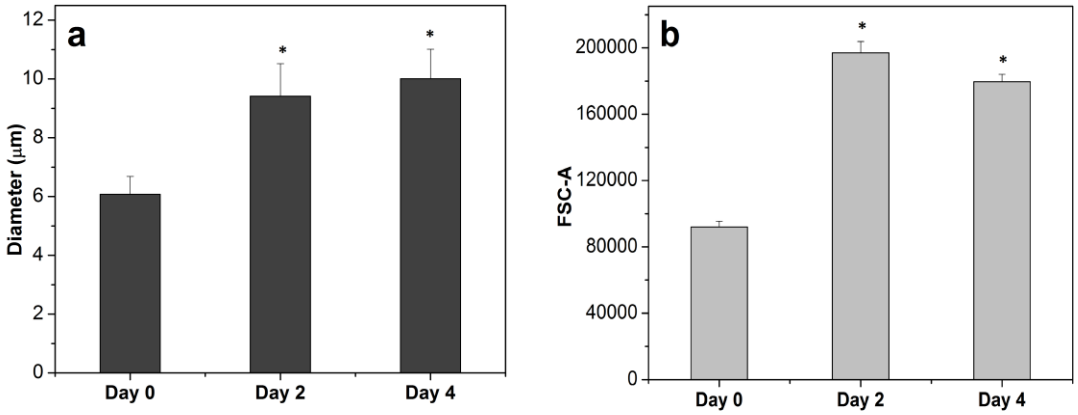
a
Diameter (μm)
0
2
4
6
8
10
12
*
*
Day 0
Day 2
Day 4
b
FSC-A
0
40000
80000
120000
160000
200000
*
*
Day 0
Day 2
Day 4

533 FIGURE 3

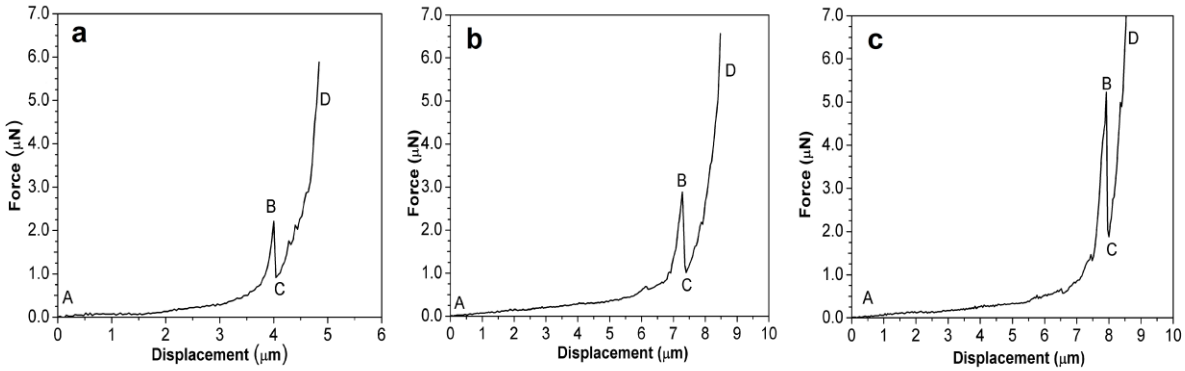

534

535

536

537

538

539

540

541

542

543

544

545 FIGURE 4

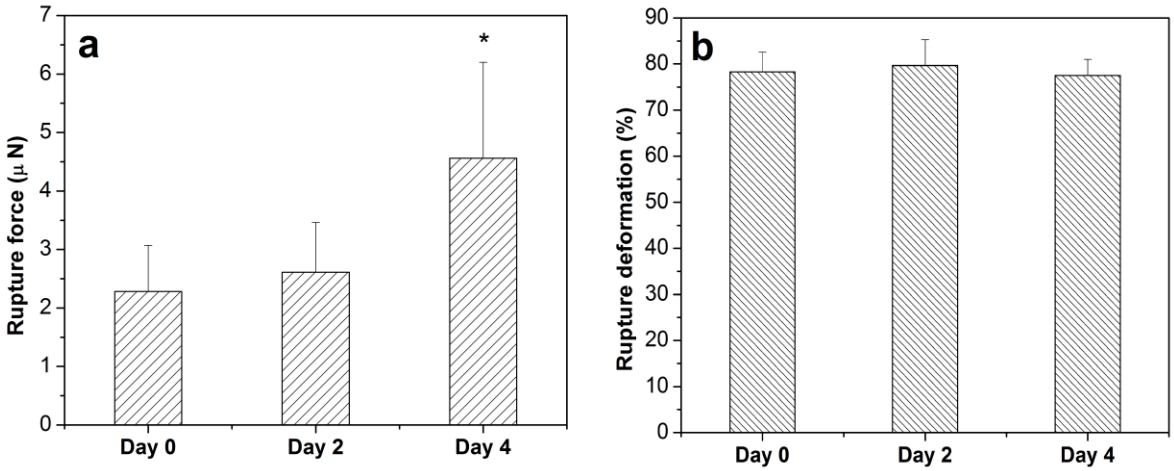

546

547

548

549

550

551

552

553

554

555

556 FIGURE 5

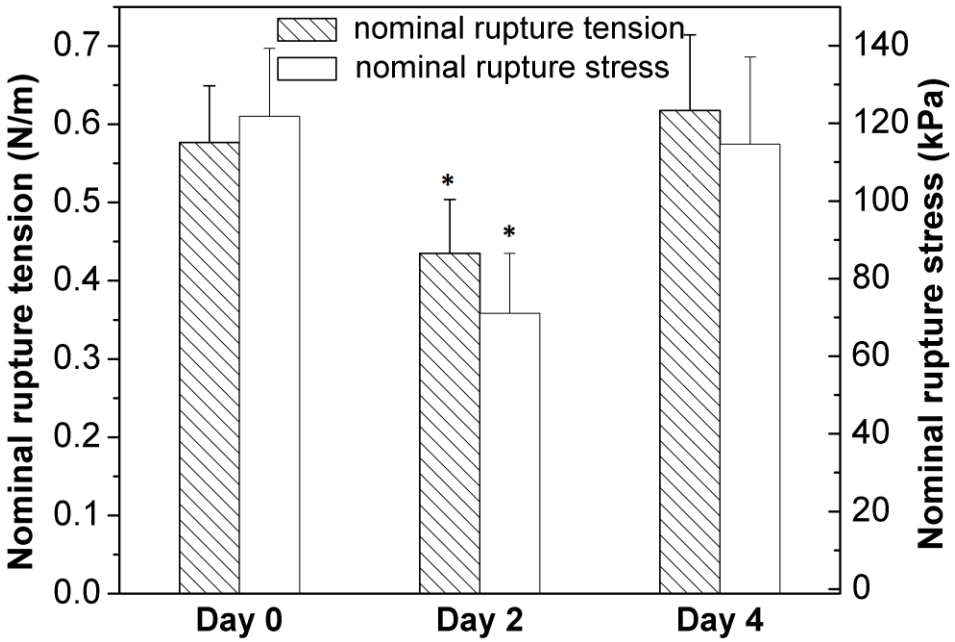

557

558

559

560

561

562

563

564

565 FIGURE 6

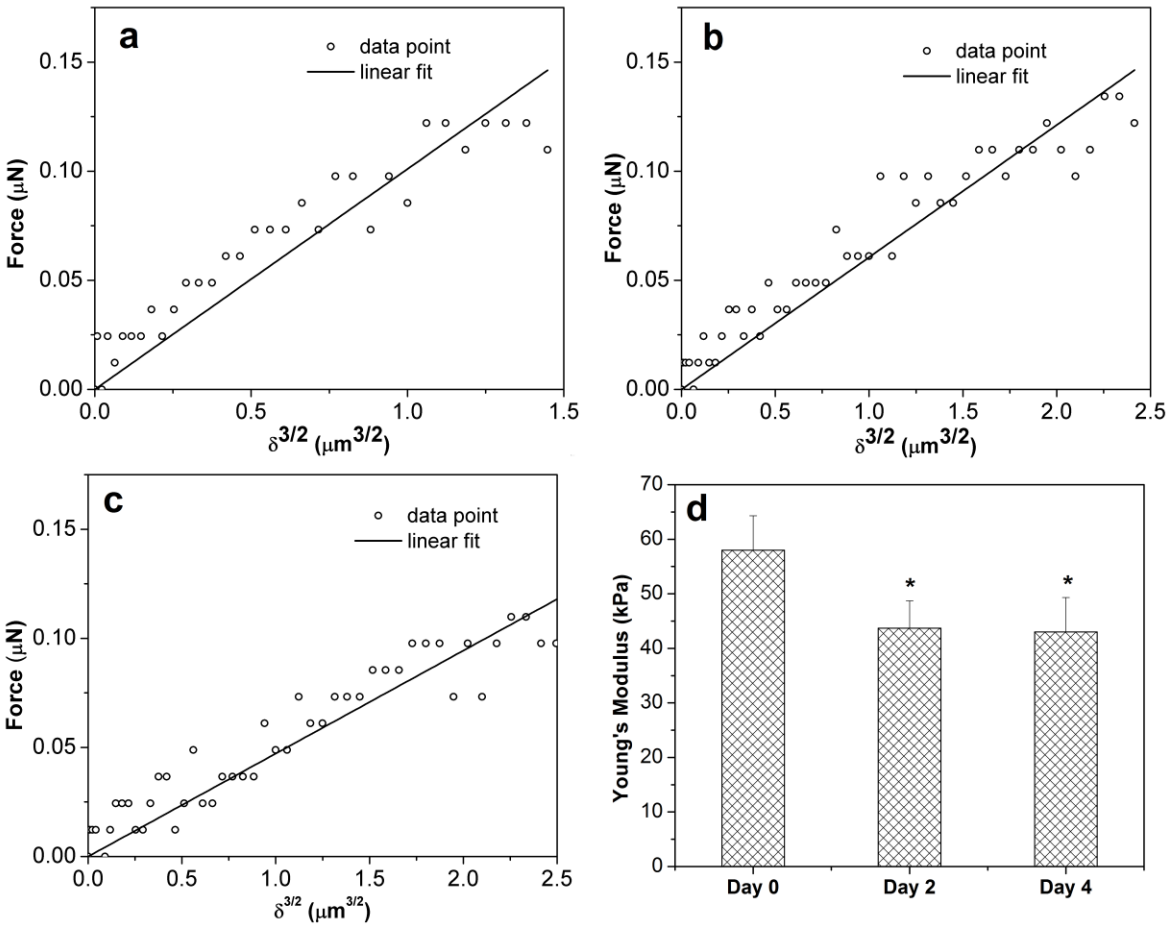

566

567

568

569

570

571

572 FIGURE 7

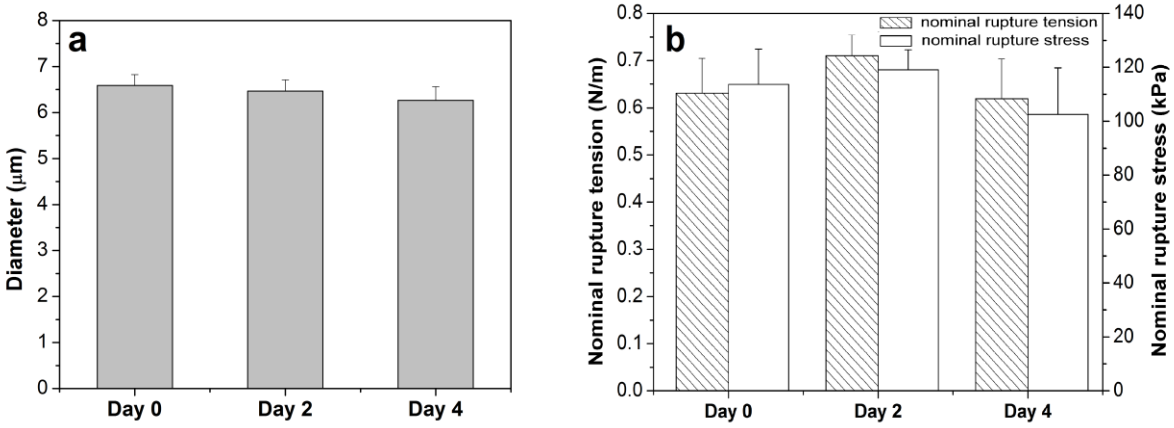

573